THE JOURNAL OF PHYSICAL CHEMISTRY C

Article

pubs.acs.org/JPCC

Size-Dependent Exciton−Phonon Coupling in CdSe Nanocrystals through Resonance Raman Excitation Profile Analysis

Chen Lin, Ke Gong, David F. Kelley, and Anne Myers Kelley*

Chemistry and Chemical Biology, University of California, Merced, 5200 North Lake Road, Merced, California 95343, United States

Supporting Information

ABSTRACT: Resonance Raman excitation profiles, including absolute Raman cross sections, have been measured for the optical phonons of organic ligand capped spherical CdSe nanocrystals with average diameters ranging from 2.6 to 5.2 nm. The absorption spectra, fundamental excitation profiles, overtone to fundamental intensity ratios, and depolarization ratio dispersion profiles are simulated using a model for the exciton−phonon coupling strengths in the various excitonic transitions that contribute to the resonance enhancement. The resonance Raman cross sections increase strongly with nanocrystal size as expected from the increased transition dipole moments (oscillator strengths) in the larger particles. However, the exciton−phonon coupling strengths, particularly for the lowest energy excitonic transition ($1S_e-1S_{3/2}$), are relatively independent of nanocrystal size over this range, perhaps decreasing slightly with increasing size. This result is consistent with calculations of exciton−phonon coupling using an atomistic model for the phonon modes and an effective mass approximation-envelope function model for the excitonic states if the electron and hole effective masses are adjusted to fit the experimental excitonic transition energies.

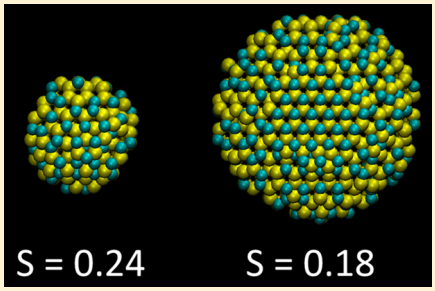

INTRODUCTION

Electron−phonon coupling (EPC) describes how the electronic energy levels of a solid are perturbed by distortion of the nuclei along a phonon coordinate. The electron−phonon coupling is defined as the magnitude of the Huang−Rhys parameter, $S = \Delta^2/2$, where Δ is the displacement between the ground- and excited-state equilibrium geometries along the phonon coordinate in units of the zero-point displacement. The strength of the coupling to phonons of various frequencies plays an important role in determining many of the spectroscopic and dynamic properties of molecules and materials. In the context of semiconductors, thermal or optical excitation of phonons perturbs the valence and/or conduction band energy levels and influences charge mobilities. In addition, relaxation processes of excited electrons, holes, and electron−hole pairs are mediated by excitation of phonons. The generic term EPC may be used to refer to the coupling of phonons to excess electrons, excess holes, or electron−hole pairs. In the present work we examine exclusively the coupling of phonons to electron−hole pairs or excitons, so the abbreviation EPC is understood to refer to exciton−phonon coupling.

In a bulk semiconductor with a perfect crystal structure, the valence and conduction band wave functions are, in principle, delocalized over the whole crystal. However, an optically created electron−hole pair becomes localized in space because of the Coulombic attraction between the opposite charges, creating an exciton. Because the hole generally has a larger effective mass than the electron, the hole is more localized and the exciton features considerable charge separation, resulting in large local electric fields. These fields couple strongly to the optical phonons of the crystal. Indeed, experimentally determined EPCs in bulk crystals of polar semiconductors are often quite large. As the crystal is made smaller than the Bohr radius of the exciton (the quantum confinement regime), the electron and hole wave functions develop a larger spatial overlap and the local electric fields generated become smaller, although they do not disappear completely because there is still charge separation at the unit cell level. At the same time, the forms of the phonons change between the bulk crystal and a nanocrystal. It is generally thought that EPC is smaller in quantum confined nanocrystals than in the bulk because of the reduced charge separation in the nanocrystal. However, there remains a great deal of disagreement among both theoretical and experimental determinations of the size dependence of EPC in polar semiconductor nanocrystals.

In this work we use resonance Raman excitation profile analysis to quantitatively assess EPC for the longitudinal optical (LO) phonon near 208 cm^{-1} in CdSe nanocrystals as a function of size. Resonance Raman spectroscopy has been widely used for studying the coupling of molecular vibrations to electronic excitations. It has also been applied to semiconductor nanocrystals, but most of these applications (with a few notable exceptions) have used simple approximations that may not be appropriate for nanocrystals having overlapping excitonic transitions. In a previous study,[1] we employed quantitative simulations of resonance Raman excitation profiles of ∼3.2 nm diameter CdSe nanocrystals and found a strong dependence of EPC strength on excitonic state. Here, we extend those studies

Received: January 25, 2015
Revised: March 16, 2015
Published: March 17, 2015

DOI: 10.1021/acs.jpcc.5b00774
J. Phys. Chem. C 2015, 119, 7491−7498

to smaller and larger sizes. Comparison of the Raman intensities and fitting parameters allows us to evaluate the effects of these changes on EPC as well as on the homogeneous and inhomogeneous contributions to the broadening of the excitonic transitions.

EXPERIMENTAL AND COMPUTATIONAL METHODS

Four sizes of CdSe nanocrystals with the wurtzite crystal structure were synthesized as described previously.[2] The samples were highly monodisperse as evidenced by the degree of structure in their absorption spectra and the width of their emission spectra and had high emission quantum yields prior to quenching by ligand exchange with hexadecanethiol[1] to allow Raman spectroscopic measurements. Ligand exchange has a negligible effect on the Raman spectra and cross sections at higher excitation energies where fluorescence does not interfere with the Raman spectra of unquenched samples.[1] The formulas of Jasieniak et al.[3] were used to determine the nanocrystal size from the wavelength of the first excitonic absorption peak and to determine the peak extinction coefficients from the wavelength and bandwidth of the first excitonic peak. Resonance Raman spectroscopy and simulations of the spectra were carried out largely as described in ref 1. Raman spectra were obtained using excitation at 457.9−514.5 nm (argon-ion laser), 532 nm (Nd laser), and 543.5−632.8 nm (He−Ne lasers). Measurements with the longer wavelength He−Ne lasers were carried out only for parallel polarization because of the weakness of the light sources, and the quantity that was calculated for the two largest NCs was $(d\sigma/d\Omega)_{\parallel}$ rather than $(d\sigma/d\Omega)_{\parallel+\perp}$ as for the two smaller samples. Absolute Raman cross sections were obtained relative to the 667 cm^{-1} line of chloroform as an internal standard as discussed previously.[1]

RESULTS

Figure 1 shows the absorption spectra of the four samples examined as well as the range of excitation wavelengths

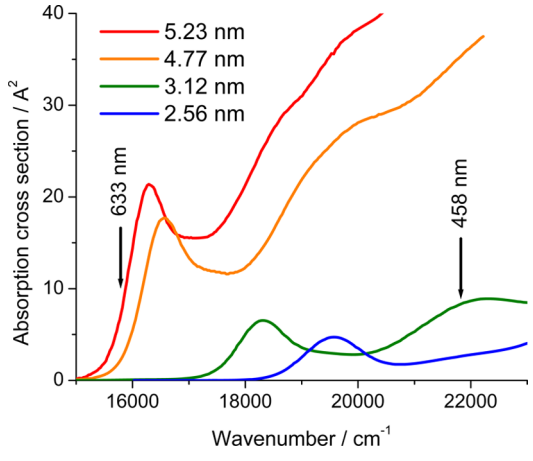

Figure 1. Absorption spectra of the four samples studied. The longest and shortest excitation wavelengths used are also indicated.

employed. The four samples have absorption maxima (following ligand exchange with hexadecanethiol) at 510, 546, 604, and 614 nm, corresponding to nanocrystal diameters of 2.56, 3.12, 4.77, and 5.23 nm, respectively. With increasing size, the absorption features shift to longer wavelengths, and there is a rapid increase in oscillator strength on a per-NC basis.

Figure 2 shows representative resonance Raman spectra of each of the four samples obtained with excitation near the

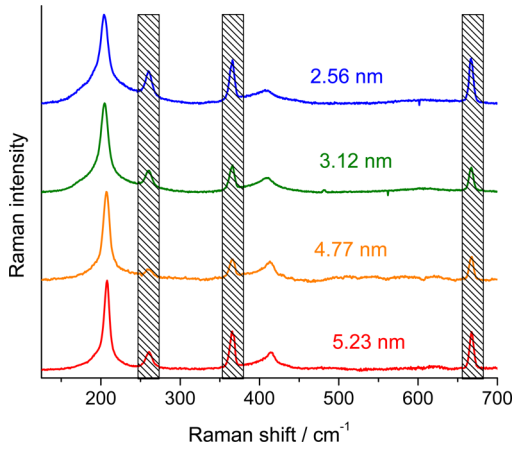

Figure 2. Resonance Raman spectra excited near the lowest excitonic absorption maximum. Excitation wavelengths are, from top to bottom, 514.5, 532, 594, and 594 nm. Shaded bars mark chloroform solvent lines whose intensity relative to that of the CdSe NCs varies with both Raman cross section and sample concentration. The spectra are parallel polarization only for the 594 nm excited samples and parallel plus perpendicular for the other two.

lowest energy absorption maximum. All four spectra show the fundamental of the longitudinal optical (LO) phonon, which shifts from about 204 cm^{-1} in the smallest NCs to about 208 cm^{-1} in the largest ones, and the first overtone of this mode. The size dependence of the LO phonon frequency is well-known.[4] The LO phonon and its overtone are broader for the smaller NCs, but otherwise the spectra are very similar. The intensity ratio of the first overtone to the fundamental is often used as a rough measure of the EPC strength in semiconductor nanocrystals. While we have stressed that the overtone to fundamental intensity ratio also depends on other factors including the homogeneous line width of the resonant excitonic transition and the degree to which multiple transitions contribute to the resonance enhancement,[5] the relative constancy of the overtone intensity with NC size under comparable resonance conditions suggests that the EPC is not strongly size dependent. The "LO phonon" in a nanocrystal is actually a superposition of multiple normal modes of similar character. While the low-frequency shoulder on the LO phonon is often identified as a "surface optical" phonon, we have shown that it is insensitive to the surface chemistry and is not well described as a surface mode.[6] For modeling purposes all of the intensity in the LO phonon region was treated as a single mode.

Figures 3−6 show the excitation profiles for the LO phonon fundamental differential Raman cross sections, LO overtone to fundamental intensity ratios, and (for the two smaller sizes) depolarization ratios as well as the fits to these data and the absorption spectra using the parameters given in Table 1 and the computational methods described in ref 1. The positions of the four lowest excitonic transitions ($1S_e-1S_{3/2}$, $1S_e-2S_{3/2}$, $1S_e-1S_{1/2}$, and $1P_e-1P_{3/2}$) were initially set to the values obtained by Norris and Bawendi through experimental low-temperature photoluminescence excitation spectroscopy.[7] These positions were then adjusted somewhat as needed to obtain an adequate fit to the absorption spectrum. A fifth transition at higher energy having zero EPC was also added.[1] The four lowest energy excitonic transitions were each split into

DOI: 10.1021/acs.jpcc.5b00774
J. Phys. Chem. C 2015, 119, 7491−7498

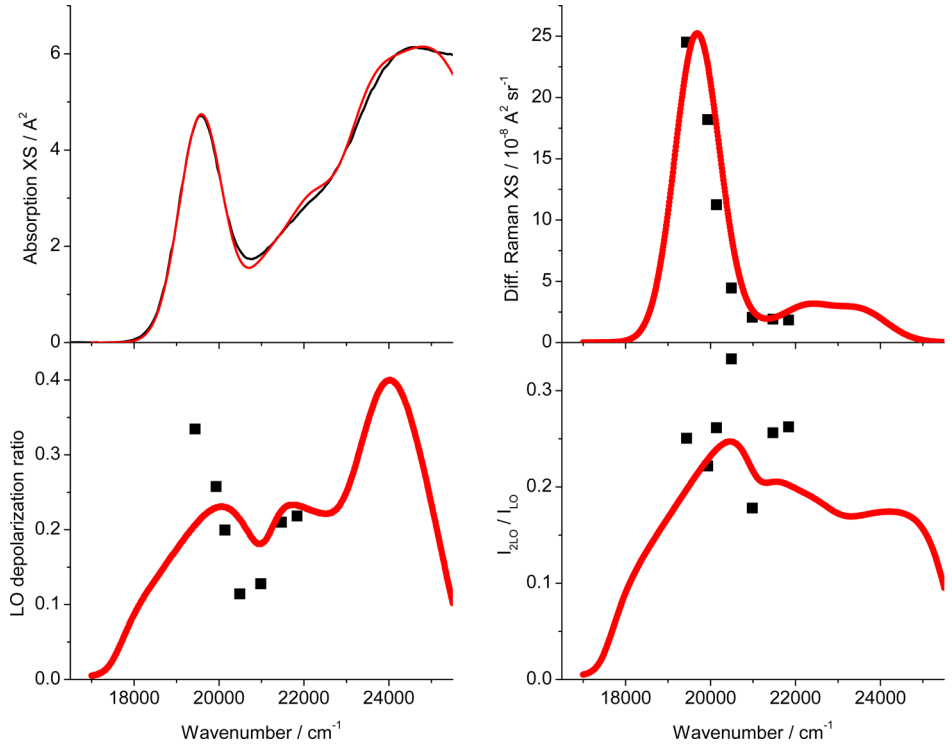

Figure 3. Experimental (black) and calculated (red) absorption cross section, LO fundamental Raman cross section, LO fundamental Raman depolarization ratio, and LO overtone to fundamental ratio for 2.56 nm CdSe NCs. Calculations use the parameters of Table 1.

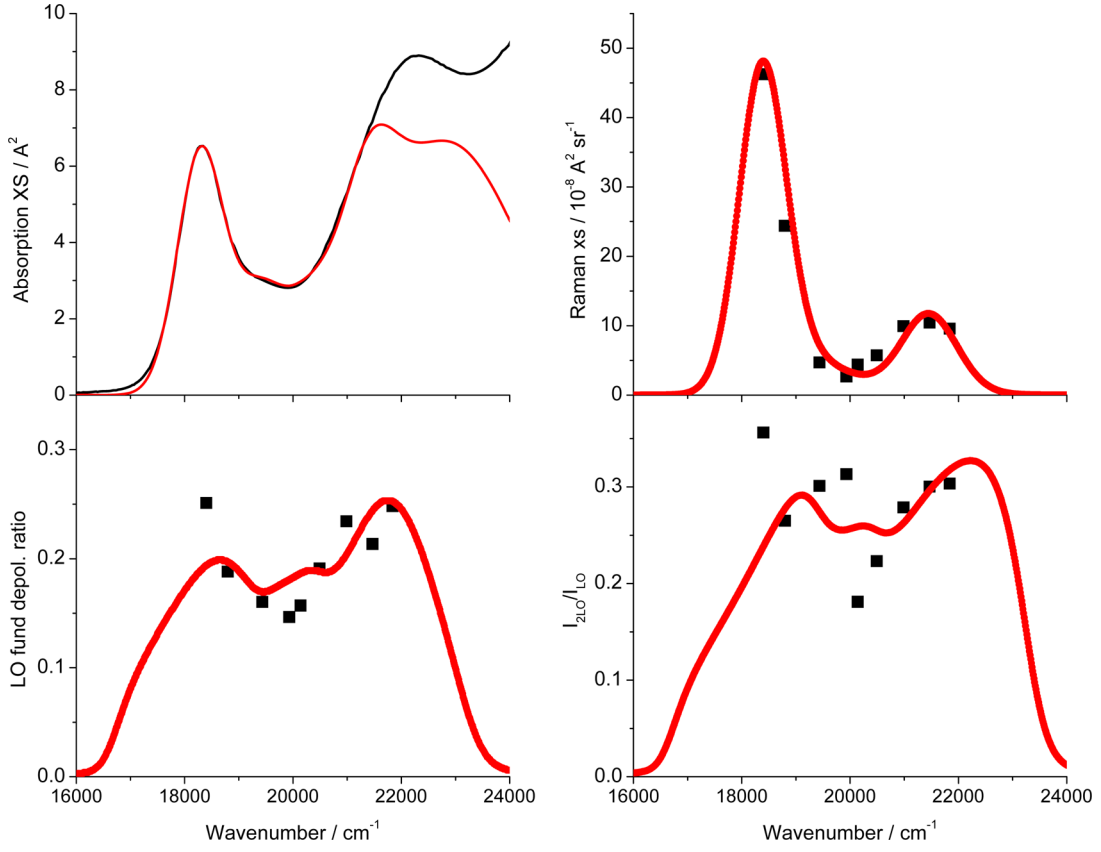

Figure 4. Same as Figure 3, for 3.12 nm CdSe NCs.

xy-polarized and *z*-polarized components having equal oscillator strengths, line widths, and EPCs, with the *xy*-polarized component initially placed 130 cm^{-1} lower in energy.[8] Each excitonic state actually has two different *xy*-polarized components ($\pm1^L$ and $\pm1^U$) in wurtzite CdSe nanocrystals, but collapsing the two into a single transition

DOI: 10.1021/acs.jpcc.5b00774
J. Phys. Chem. C 2015, 119, 7491−7498

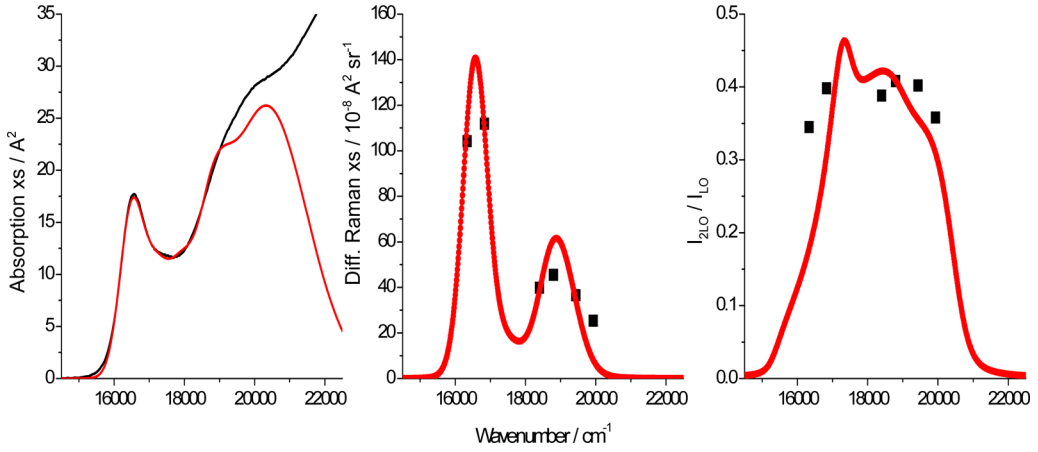

Figure 5. Same as Figure 3, for 4.77 nm diameter NCs. Raman data are for parallel polarization only.

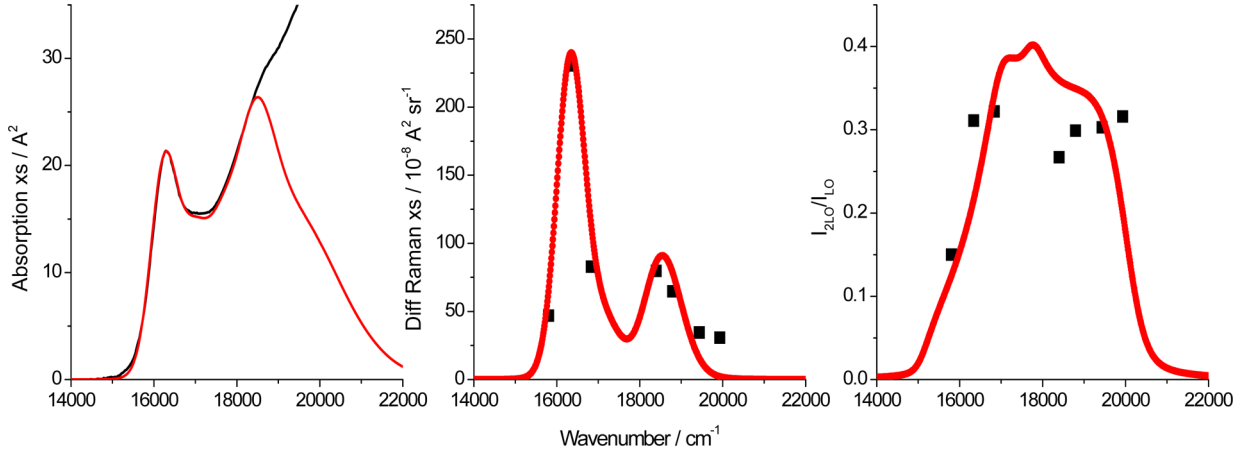

Figure 6. Same as Figure 3, for 5.23 nm diameter NCs. Raman data are for parallel polarization only.

Table 1. Parameters (Excitonic Energy *E*, Homogeneous Line Width Γ, Transition Dipole Length *M*, and LO Phonon Huang–Rhys Parameter *S*) for Modeling Absorption Spectra and Raman Intensities

transition (polarization)	property	2.56 nm	3.12 nm	4.77 nm	5.23 nm
$1S_e-1S_{3/2}$ (xy/z)	E/cm^{-1}	19475/19775	18220/18450	16460/16595	16210/16345
	Γ/cm^{-1}	360	290	330	290
	M/Å	1.27	1.40	2.08	2.26
	S	0.24	0.21	0.21	0.18
$1S_e-2S_{3/2}$ (xy/z)	E/cm^{-1}	21035/21335	19310/19540	17180/17315	16940/17075
	Γ/cm^{-1}	500	400	400	290
	M/Å	0.68	0.85	1.52	1.52
	S	0.24	0.21	0.21	0.18
$1S_e-1S_{1/2}$ (xy/z)	E/cm^{-1}	22045/22355	20240/20470	17870/18005	17590/17725
	Γ/cm^{-1}	500	400	400	300
	M/Å	0.80	0.67	1.37	1.25
	S	0.24	0.21	0.21	0.18
$1P_e-1P_{3/2}$ (xy/z)	E/cm^{-1}	23290/23790	21272/21622	18700/19100	18350/18650
	Γ/cm^{-1}	500	400	400	450
	M/Å	0.75	0.95	1.70	1.90
	S	0.24	0.41	0.61	0.61
unassigned (z)	E/cm^{-1}	24900	22800	20300	19100
	Γ/cm^{-1}	3000	3000	2600	2800
	M/Å	3.6	3.90	7.60	6.40
	S	0	0	0	0
inhomogeneous (Gaussian) fwhm/cm^{-1}		1060	895	655	648

had little effect on the results of the fits. The splitting between the *xy*-polarized and *z*-polarized fine-structure states was varied somewhat in order to better fit the Raman depolarization dispersion curves (*vide infra*), and the positions, line widths,

DOI: 10.1021/acs.jpcc.5b00774
J. Phys. Chem. C 2015, 119, 7491−7498

oscillator strengths, and EPCs of all transitions were varied to achieve an overall best fit to all of the Raman and absorption data. The overtone intensities and depolarization ratios carry considerably larger experimental uncertainties than the absorption spectra and fundamental Raman cross sections, as reflected in the poorer fits to the more scattered data points. The final parameters are summarized in Table 1.

The Huang–Rhys parameter was assumed to be the same for the three lowest energy excitonic resonances of a given sample ($1S_e-1S_{3/2}$, $1S_e-2S_{3/2}$, and $1S_e-1S_{1/2}$) but was allowed to be different for the $1P_e-1P_{3/2}$ and was set to zero for the unassigned highest energy transition.[1] Simple calculations of the type described in ref 6 and Supporting Information suggest that the EPC should be larger for the $1S_e-2S_{3/2}$ transition than for the $1S_e-1S_{3/2}$, but attempting to use a significantly larger Huang–Rhys parameter for the $1S_e-2S_{3/2}$ transition degraded the quality of the fits. The best fits to the data were obtained with the low-energy Huang–Rhys parameter in the range from 0.18 to 0.24 for all four samples, increasing very slightly with decreasing NC size. In light of the uncertainties in the data and the fitting process, we are unwilling to conclude that there is any size dependence of the EPC; it is, in any case, not very strong over the significant size range explored here.

DISCUSSION

The magnitude and size dependence of EPC in II–VI nanocrystals has been addressed both experimentally and theoretically by many workers without any consensus being reached. As summarized in ref 9, reported Huang–Rhys parameters for the LO phonon of similar sized CdSe nanocrystals span nearly 2 orders of magnitude, and the EPC strength has been reported to increase,[10] decrease,[11,12] remain approximately constant,[4,13−15] or change nonmonotonically[16−18] with increasing NC size. Only a few papers have addressed the dependence of EPC on excitonic state.[1,15,19] Furthermore, the magnitude of EPC even in the bulk crystal is not well determined. Alivisatos et al.[20] gave values for bulk CdSe of $\Delta = 2.93$ based on the theoretical expression of Merlin[21] and $\Delta = 3.6$ based on the overtone intensity in the emission spectrum of Gross et al.,[22] but neither the experimental data nor the overtone intensity analysis is very clear. Subsequent papers quoted[13,23] a Huang–Rhys parameter of $S \sim 10$ based on this work. The photon echo study by Mittleman et al.[18] quoted a bulk value of $\Delta = 0.63$ citing ref 24, but that paper actually gave only $S \leq 0.2$ in the bulk, citing the exciton absorption spectra of Voigt et al.[25] Valerini et al.[26] cited the same Voigt paper[25] for an LO phonon–exciton coupling coefficient of $\Gamma_{LO} \sim 100$ meV ($\sim$800 cm^{-1}), corresponding to a much larger S value. Nomura and Kobayashi calculated Huang–Rhys parameters for bulk CdSe varying from $S = 0.38$ to $S = 1.4$ for hole effective masses from 0.45 to 1.0.[17] Note that while the theoretical estimates are for 1S exciton states,[17,21] many of the experiments involve resonance with ill-defined superpositions of transitions.

In a polar crystal such as CdSe there are two principal sources of EPC: polar coupling and deformation potential coupling. The polar (Fröhlich) coupling is a long-range interaction arising from the interaction between the electric field generated by the exciton and the oscillating dipole moment created by the phonon. The deformation potential coupling is a more local interaction arising from the changes in bond order induced by electronic excitation. For optical phonons, while both mechanisms may contribute, the polar coupling is expected to be much more important (see Supporting Information). In a bulk crystal, the exciton consists of an electron and hole bound by Coulombic interaction. The hole is more localized than the electron because of its greater effective mass. The smaller spatial extent of the hole results in a significant radial electric field and hence strong coupling to optical phonons that have wavelengths comparable to the Bohr radius of the exciton. In a nanocrystal whose physical size is smaller than the Bohr radius, there are two considerations that determine the magnitude of the EPC. First, although the electron and hole are expected to have more similar spatial distributions than in the bulk, spill-out of the electron wave function past the particle surface results in a radial electric field that induces EPC through the Fröhlich mechanism.[27] The extent of spill-out is size dependent, and hence so is this factor in determining the Huang–Rhys parameter. Second, because Δ is in units of the dimensionless normal coordinate q, the magnitude of the Huang–Rhys parameter also depends on the magnitude of the zero-point displacement of the phonon mode. The number of unit cells involved in any particular phonon normal mode tends to increase with particle size. Since the energies are constant at about 208 cm^{-1}, the magnitudes of the zero-point displacements tend to decrease with particle size. These two effects go in opposite directions: the electric field dependence tends to make the EPC increase with decreasing particle size while the phonon delocalization has the opposite effect. Below we present quantitative calculations that show that these effects almost cancel and the calculated EPC is nearly size independent over the size range studied, in agreement with the experimental result.

Calculations were carried out using an effective mass approximation envelope function method,[6] with electron–hole Coulombic interaction included (see Supporting Information and Table S1). It is well-known that with bulk values for the electron and hole effective masses ($m_e^* = 0.13m_0$ and $m_h^* = 0.45m_0$)[28] and reasonable values for the potential step at the edge of the particle (2–4 eV), a simple effective mass model overpredicts the 1S–1S transition energy and the 1S–1S/1S–2S energy splitting.[29] For our calculations of size-dependent EPC, we set the potential step at the edge of the particle to 2.5 eV for both electrons and holes and chose the electron and hole effective masses to correctly reproduce the energies of the first two excitonic transitions as a function of NC size.[29] The effective masses used varied from $m_e^* = 0.095m_0$ for 1.4 nm radius NCs to $m_e^* = 0.14m_0$ for 2.6 nm radius NCs. A large but size-independent hole effective mass of $m_h^* = 2.9m_0$ was used. With these parameters, we calculated electron and hole wave functions and hence the magnitude of the exciton-induced electric field in the particle. Using phonon modes calculated as described in refs 6 and 30 with the force field described in Supporting Information, a nearly size-independent EPC for the LO phonons is obtained (see Table S1). This is consistent with the experimental results of Table 1. The calculated electric field inside the NC is larger for the smaller radius, but this does not give rise to increased EPC because the phonon normal coordinate involves smaller Cartesian displacements of the atoms when the number of atoms is larger. We note that both the transition energies and EPCs depend on the calculated extent of electron quantum confinement. If size independent effective masses are used, significantly larger transition energies (not agreeing with the experimental values) and EPCs are calculated for the smaller particles. It should be noted that all of these calculations assume neutral nanocrystals. Preliminary

DOI: 10.1021/acs.jpcc.5b00774
J. Phys. Chem. C 2015, 119, 7491−7498

calculations indicate that a localized surface charge increases EPC by perturbing the electron and hole wave functions and that the magnitude of the effect depends on NC size. This will be addressed more fully in work in progress on EPC in core−shell NCs.

The large number of excitonic transitions within a small frequency range in these materials necessitates a large number of parameters in the calculations that model the absorption and Raman data. The use of existing theoretical and spectroscopic data to constrain many of these parameters was described in our previous work.[1] However, few of the parameters are extremely well determined by either theory or experiment, and there are many somewhat different, and still reasonable, parameter sets that reproduce the data about equally well. In general, the parameters describing the higher energy transitions become increasingly ill-defined because of the strong overlap among transitions. The parameters related to the lowest energy, $1S_e-1S_{3/2}$ transition are the most accurately determined because this transition is the most spectrally isolated. The transition dipole moment and the total (inhomogeneous plus homogeneous) excitonic width are reasonably well-defined by the low-energy region of the absorption spectrum, although the required broadening depends slightly on the assumed magnitude of the fine-structure splitting. The resonance Raman cross section for the LO fundamental then depends on both the fraction of the broadening that is homogeneous and the magnitude of the EPC (smaller EPC can be compensated by a smaller homogeneous width), so the Raman fundamental intensity alone cannot be used to determine the EPC even for a single excitonic resonance. The fundamental and overtone intensities together allow both of these parameters to be determined with reasonable precision,[5] but there is still some uncertainty arising from the poorly defined fine-structure splitting and the non-negligible contribution to the Raman intensities from higher lying transitions that slightly overlap the $1S_e-1S_{3/2}$.

In wurtzite CdSe, the $1S_e-1S_{3/2}$ exciton is split into five different fine-structure energy levels by the asymmetry of the wurtzite lattice and the electron−hole exchange interaction. Three of these levels, one *z*-polarized and two *xy*-polarized, are "bright" and the other two are "dark".[8] As in our previous work, we approximated this situation by treating each excitonic transition as a pair of transitions, one *xy*-polarized and one *z*-polarized, with the *xy*-transition carrying twice the oscillator strength of the *z*-transition and the *xy*-transition slightly lower in energy. The *xy*/*z* splitting was assumed constant for all S−S excitons in a given size NC but was assumed to increase slightly with decreasing NC size as shown in Table 1. A larger splitting in the nominal $1P_e-1P_{3/2}$ transition was used for all samples. To our knowledge the fine-structure splitting has been neither measured nor calculated for higher energy excitonic states. It is, however, clear that the actual NCs are not all perfectly spherical, and any shape asymmetry will not only affect the fine-structure splittings but also break the degeneracy of the P_x, P_y, and P_z electron and hole envelope functions. The larger splitting required in the simulations may therefore have little or nothing to do with the fine structure but may simply reflect the loss of degeneracy of the P-type envelope functions. This analysis assumes that the low-intensity, high-EPC transition is the $1P_e-1P_{3/2}$, but a highly anisotropic transition dipole would also be expected for a surface state transition.

The experimental depolarization ratio dispersion curves of Figures 3 and 4 both show a clear minimum near the minimum in the absorbance (near 20 700 and 20 000 cm^{-1}, respectively, for the 2.56 and 3.12 nm NCs) and increase at both higher and lower excitation energies. This pattern is observed not only in these two samples but also in zincblende NCs of similar sizes (data not shown) as well as in the much earlier experiments by Shiang et al. on wurtzite CdSe NCs.[31] Those authors interpreted their data in terms of each major excitonic transition being either *z*-polarized or *xy*-polarized, but this is inconsistent with what is now known about the fine-structure splitting of each exciton.[8] Our simulations show that because of the constructive or destructive interferences between the *z*-polarized and *xy*-polarized components of the Raman polarizability,[1,32] the dependence of the depolarization ratio on excitation wavelength is a fairly sensitive function of the assumed splitting between *z*-polarized and *xy*-polarized transitions. While we were able to model the general shapes of the dispersion curves (Figures 3 and 4), we were not able to obtain the relatively high depolarization ratios at the lowest excitation energies, nor were the results improved by assuming slightly oblate or prolate shapes together with the energies and oscillator strengths of the fine-structure components for these shapes.[8] The discrepancy may result from large anisotropies induced by surface charges, which would perturb both the fine-structure states and the envelope functions in ways that are difficult to model.

The assignments of the four lowest-energy excitonic transitions in Table 1 are taken from the work of Norris and Bawendi.[7] However, the oscillator strength of the third transition, assigned as the $1S_e-1S_{1/2}$, does not follow the predicted trend. According to calculations[7] that include the mixing between the S-type and D-type envelope functions,[33,34] in larger nanocrystals the $1S_{1/2}$ hole state has largely D character and therefore has a small overlap with the 1S electron state, and the intensity (oscillator strength) of the $1S_e-1S_{1/2}$ transition is expected to decrease rapidly with increasing size. The strengths of the weaker transitions are difficult to determine accurately because of their strong overlap, but we were not able to fit the data for the larger QDs with a $(1S_e-1S_{1/2}):(1S_e-1S_{3/2})$ intensity ratio smaller than that used for the 3.12 nm particles. Therefore, this assignment remains somewhat questionable.

The region of the $1P_e-1P_{3/2}$ excitation also warrants further discussion. We have placed two transitions in this region: one with relatively large EPC and an oscillator strength somewhat lower than that of the $1S_e-1S_{3/2}$ and another very broad band with zero EPC and an oscillator strength much higher than that of the $1S_e-1S_{3/2}$. As discussed previously,[1] this is required to simultaneously fit the relatively high absorbance, high overtone intensity, and low fundamental Raman cross section in this region. The broad band with large oscillator strength must represent more than one transition, but it is not clear whether the $1P_e-1P_{3/2}$ should be assigned as the high-EPC transition or as part of the low-EPC band. Within the simple particle in a sphere approximation for the electron and hole wave functions, the only strongly allowed excitonic transitions should be those that involve the same principal quantum number and angular momentum for the electron and the hole, and because of the degeneracy of the P states, the $1P_e-1P_{3/2}$ should have 3 times the oscillator strength of the $1S_e-1S_{3/2}$. (The calculations of Ekimov et al. indicate equal oscillator strengths for these two transitions,[35] but it is not clear whether the degeneracy of the P functions was taken into account.) The femtosecond pump−probe studies of Sagar et al. also show reduced EPC for the

DOI: 10.1021/acs.jpcc.5b00774
J. Phys. Chem. C 2015, 119, 7491−7498

higher-lying transitions (e.g., $1P_e-1P_{3/2}$) relative to the $1S_e-1S_{3/2}$.[19] Both pieces of data suggest that the $1P_e-1P_{3/2}$ is part of the broad transition with near-zero EPC.

Essentially all theoretical treatments of the effect of NC size on EPC have focused entirely on the size dependence of the electronic excitations and not on any size dependence of the form of the phonons. Atomistic simulations of the phonons using empirical force fields[6,30] indicate that the optical phonons of nanocrystals are quite different from those of the bulk; while all "LO"-type phonons look about the same at the unit cell level, they are somewhat localized to different regions within the NC because of the modest degree of surface reconstruction in the NC. The phonon normal modes in a NC have neither well-defined wavevectors nor well-defined angular momenta, and many different LO-type phonons, some fairly delocalized and others localized to fairly small regions of the NC, all contribute to the EPC. While we report a single value for the LO phonon Huang−Rhys parameter, it should be recognized that this actually refers to the sum of the Huang−Rhys parameters for a number of nearly degenerate phonon modes.

CONCLUSIONS

The magnitude of electron−phonon coupling between the longitudinal optical phonon and the lowest energy excitonic transition of wurtzite CdSe quantum dots exhibits only weak size dependence in the 2.6−5.2 nm diameter range. Resonance Raman intensity analysis yields a Huang−Rhys parameter of 0.18−0.24 throughout this size range. The experimental result agrees with calculations combining an effective mass envelope function model for the excitonic states with atomistic force field calculations of the phonons if the effective masses are adjusted to give the correct excitonic energies.

ASSOCIATED CONTENT

Supporting Information

Details of the calculations of electron−phonon coupling for two sizes of CdSe nanocrystals. This material is available free of charge via the Internet at http://pubs.acs.org.

AUTHOR INFORMATION

Corresponding Author

*Tel 209-228-4345; e-mail amkelley@ucmerced.edu (A.M.K.).

Notes

The authors declare no competing financial interest.

ACKNOWLEDGMENTS

This work was supported by NSF Grant CHE-1112192.

REFERENCES

(1) Baker, J. A.; Kelley, D. F.; Kelley, A. M. Resonance Raman and Photoluminescence Excitation Profiles and Excited-State Dynamics in CdSe Nanocrystals. *J. Chem. Phys.* **2013**, *139*, 024702.

(2) Gong, K.; Zeng, Y.; Kelley, D. F. Extinction Coefficients, Oscillator Strengths, and Radiative Lifetimes of CdSe, CdTe, and CdTe/CdSe Nanocrystals. *J. Phys. Chem. C* **2013**, *117*, 20268−20279.

(3) Jasieniak, J.; Smith, L.; van Embden, J.; Mulvaney, P.; Califano, M. Re-Examination of the Size-Dependent Absorption Properties of CdSe Quantum Dots. *J. Phys. Chem. C* **2009**, *113*, 19468−19474.

(4) Dzhagan, V. M.; Valakh, M. Y.; Raevskaya, A. E.; Stroyuk, A. L.; Kuchmiy, S. Y.; Zahn, D. R. T. Size Effects on Raman Spectra of Small CdSe Nanoparticles in Polymer Films. *Nanotechnology* **2008**, *19*, 305707.

(5) Kelley, A. M. Resonance Raman Overtone Intensities and Electron-Phonon Coupling Strengths in Semiconductor Nanocrystals. *J. Phys. Chem. A* **2013**, *117*, 6143−6149.

(6) Lin, C.; Kelley, D. F.; Rico, M.; Kelley, A. M. The "Surface Optical" Phonon in CdSe Nanocrystals. *ACS Nano* **2014**, *8*, 3928−3938.

(7) Norris, D. J.; Bawendi, M. G. Measurement and Assignment of the Size-Dependent Optical Spectrum in CdSe Quantum Dots. *Phys. Rev. B* **1996**, *53*, 16338−16346.

(8) Efros, A. L.; Rosen, M.; Kuno, M.; Nirmal, M.; Norris, D. J.; Bawendi, M. Band-Edge Exciton in Quantum Dots of Semiconductors With a Degenerate Valence Band: Dark and Bright Exciton States. *Phys. Rev. B* **1996**, *54*, 4843−4856.

(9) Kelley, A. M. Electron−Phonon Coupling in CdSe Nanocrystals. *J. Phys. Chem. Lett.* **2010**, *1*, 1296−1300.

(10) Rodriguez-Suarez, R.; Menendez-Proupin, E.; Trallero-Giner, C.; Cardona, M. Multiphonon Resonant Raman Scattering in Nanocrystals. *Phys. Rev. B* **2000**, *62*, 11006−11016.

(11) Scamarcio, G.; Spagnolo, V.; Ventruti, G.; Lugara, M.; Righini, G. C. Size Dependence of Electron-LO-Phonon Coupling in Semiconductor Nanocrystals. *Phys. Rev. B* **1996**, *53*, R10489−R10492.

(12) Takagahara, T. Electron-Phonon Interactions and Excitonic Dephasing in Semiconductor Nanocrystals. *Phys. Rev. Lett.* **1993**, *71*, 3577−3580.

(13) Klein, M. C.; Hache, F.; Ricard, D.; Flytzanis, C. Size Dependence of Electron-Phonon Coupling in Semiconductor Nanospheres: The Case of CdSe. *Phys. Rev. B* **1990**, *42*, 11123−11132.

(14) Norris, D. J.; Efros, A. L.; Rosen, M.; Bawendi, M. G. Size Dependence of Exciton Fine Structure in CdSe Quantum Dots. *Phys. Rev. B* **1996**, *53*, 16347−16354.

(15) Sagar, D. M.; Cooney, R. R.; Sewall, S. L.; Dias, E. A.; Barsan, M. M.; Butler, I. S.; Kambhampati, P. Size Dependent, State-Resolved Studies of Exciton-Phonon Couplings in Strongly Confined Semiconductor Quantum Dots. *Phys. Rev. B* **2008**, *77*, 235321.

(16) Melnikov, D. V.; Fowler, W. B. Electron-Phonon Interaction in a Spherical Quantum Dot with Finite Potential Barriers: The Fröhlich Hamiltonian. *Phys. Rev. B* **2001**, *64*, 245320.

(17) Nomura, S.; Kobayashi, T. Exciton-LO-Phonon Couplings in Spherical Semiconductor Microcrystallites. *Phys. Rev. B* **1992**, *45*, 1305−1316.

(18) Mittleman, D. M.; Schoenlein, R. W.; Shiang, J. J.; Colvin, V. L.; Alivisatos, A. P.; Shank, C. V. Quantum Size Dependence of Femtosecond Electronic Dephasing and Vibrational Dynamics in CdSe Nanocrystals. *Phys. Rev. B* **1994**, *49*, 14435−14447.

(19) Sagar, D. M.; Cooney, R. R.; Sewall, S. L.; Kambhampati, P. State-Resolved Exciton-Phonon Couplings in CdSe Semiconductor Quantum Dots. *J. Phys. Chem. C* **2008**, *112*, 9124−9127.

(20) Alivisatos, A. P.; Harris, T. D.; Carroll, P. J.; Steigerwald, M. L.; Brus, L. E. Electron-Vibration Coupling in Semiconductor Clusters Studied by Resonance Raman Spectroscopy. *J. Chem. Phys.* **1989**, *90*, 3463−3468.

(21) Merlin, R.; Guntherodt, G.; Humphreys, R.; Cardona, M.; Suryanarayanan, R.; Holtzberg, F. Multiphonon Processes in YbS. *Phys. Rev. B* **1978**, *17*, 4951−4958.

(22) Gross, E.; Permogorov, S.; Morozenko, Y.; Kharlamov, B. Hot-Exciton Luminescence in CdSe Crystals. *Phys. Status Solidi B* **1973**, *59*, 551−560.

(23) Baranov, A. V.; Rakovich, Y. P.; Donegan, J. F.; Perova, T. S.; Moore, R. A.; Talapin, D. V.; Rogach, A. L.; Masumoto, Y.; Nabiev, I. Effect of ZnS Shell Thickness on the Phonon Spectra in CdSe Quantum Dots. *Phys. Rev. B* **2003**, *68*, 165306.

(24) Woggon, U.; Gaponenko, S.; Langbein, W.; Uhrig, A.; Klingshirn, C. Homogeneous Linewidth of Confined Electron-Hole Pair States in II-VI Quantum Dots. *Phys. Rev. B* **1993**, *47*, 3684−3689.

(25) Voigt, J.; Spiegelberg, F.; Senoner, M. Band Parameters of CdS and CdSe Single Crystals Determined from Optical Exciton Spectra. *Phys. Status Solidi B* **1979**, *91*, 189−199.

(26) Valerini, D.; Creti, A.; Lomascolo, M.; Manna, L.; Cingolani, R.; Anni, M. Temperature Dependence of the Photoluminescence

DOI: 10.1021/acs.jpcc.5b00774
J. Phys. Chem. C 2015, 119, 7491−7498

Properties of Colloidal CdSe/ZnS Core/Shell Quantum Dots Embedded in a Polystyrene Matrix. *Phys. Rev. B* **2005**, *71*, 235409.
(27) Steigerwald, M. L.; Brus, L. E. Semiconductor Crystallites: A Class of Large Molecules. *Acc. Chem. Res.* **1990**, *23*, 183−188.
(28) Wheeler, R. G.; Dimmock, J. O. Exciton Structure and Zeeman Effects in Cadmium Selenide. *Phys. Rev.* **1962**, *125*, 1805−1815.
(29) Gong, K.; Martin, J. E.; Shea-Rohwer, L. E.; Lu, P.; Kelley, D. F. Radiative Lifetimes of Zincblende CdSe/CdS Quantum Dots. *J. Phys. Chem. C* **2015**, *119*, 2231−2238.
(30) Kelley, A. M. Electron-Phonon Coupling in CdSe Nanocrystals from an Atomistic Phonon Model. *ACS Nano* **2011**, *5*, 5254−5262.
(31) Shiang, J. J.; Kadavanich, A. V.; Grubbs, R. K.; Alivisatos, A. P. Symmetry of Annealed Wurtzite CdSe Nanocrystals: Assignment to the C_{3v} Point Group. *J. Phys. Chem.* **1995**, *99*, 17417−17422.
(32) Sension, R. J.; Strauss, H. L. Comparison of Experiment and Theory for the Resonance Raman Spectrum of I_2 in Solution. I. The Raman Excitation Profile of I_2 in n-Hexane. *J. Chem. Phys.* **1986**, *85*, 3791−3806.
(33) Efros, A. L. Luminescence Polarization of CdSe Microcrystals. *Phys. Rev. B* **1992**, *46*, 7448−7458.
(34) Grigoryan, G. B.; Kazaryan, E. M.; Efros, A. L.; Yazeva, T. V. Quantized Holes and the Absorption Edge in Spherical Semiconductor Microcrystals with a Complex Valence Band Structure. *Sov. Phys. Solid State* **1990**, *32*, 1031−1035.
(35) Ekimov, A. I.; Hache, F.; Schanne-Klein, M. C.; Ricard, D.; Flytzanis, C.; Kudryavtsev, I. A.; Yazeva, T. V.; Rodina, A. V. Absorption and Intensity-Dependent Photoluminescence Measurements on CdSe Quantum Dots: Assignment of the First Electronic Transition. *J. Opt. Soc. Am. B* **1993**, *10*, 100−107.

DOI: 10.1021/acs.jpcc.5b00774
J. Phys. Chem. C 2015, 119, 7491−7498